Fusion Engineering and Design 121 (2017) 159–166

Contents lists available at ScienceDirect

Fusion Engineering and Design

journal homepage: www.elsevier.com/locate/fusengdes

Research paper

Effects of Y_2O_3, La_2O_3 and CeO_2 additions on microstructure and mechanical properties of 14Cr-ODS ferrite alloys produced by spark plasma sintering

Zhengyuan Li, Zheng Lu*, Rui Xie, Chenyang Lu, Yingnan Shi, Chunming Liu

Key Laboratory for Anisotropy and Texture of Materials (Ministry of Education), School of Materials Science and Engineering, Northeastern University, Shenyang, China

HIGHLIGHTS

- The 14Cr-ODS ferritic alloys with Y_2O_3, La_2O_3 and CeO_2 additions were produced by mechanical alloying (MA) and spark plasma sintering (SPS).
- High-density nanoscale $Y_2Ti_2O_7$, $La_2Ti_2O_7$ and $Ce_2Ti_2O_7$ oxides were identified by high resolution transmission electron microscope (HRTEM) in three kinds of 14Cr-ODS steels, respectively.
- The contribution of nanoscale oxides to yield strength is dominating.

GRAPHICAL ABSTRACT

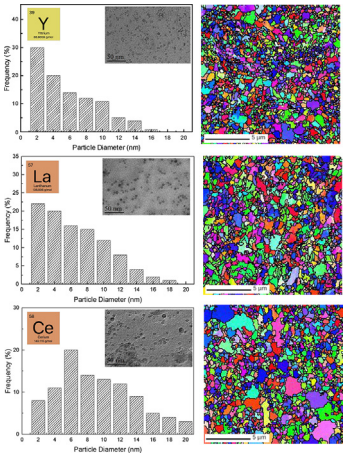

ARTICLE INFO

Article history:
Received 13 February 2017
Received in revised form 20 May 2017
Accepted 29 June 2017

Keywords:
Spark plasma sintering (SPS)
14Cr-ODS alloy
Microstructure
Nanoscale oxides
Yield strength

ABSTRACT

14Cr oxide dispersion strengthened (ODS) alloys with the additions of Y_2O_3, La_2O_3 and CeO_2 (denoted as 14Y, 14L, and 14C), respectively, were produced by mechanical alloying (MA) and spark plasma sintering (SPS). The effects of Y_2O_3, La_2O_3 and CeO_2 on the microstructures of 14Cr-ODS alloys were characterized by using electron backscattered diffraction (EBSD) and transmission electron microscopy (TEM), and the mechanical properties were evaluated using microhardness and tensile test. The results showed that ultra-fine grains with random crystallographic orientations are formed in the SPSed ODS alloys. High-density nanoscale $Y_2Ti_2O_7$ oxides in 14Y, $La_2Ti_2O_7$ oxides in 14L and $Ce_2Ti_2O_7$ oxides in 14C are observed, respectively. The average oxide size increases while the areal number density of them decreases in order of 14Y, 14L and 14C. The yield strength of 14Y alloy is higher than that of 14L and 14C. The contributions of Hall-Petch strengthening and dispersion strengthening to yield strength in the three kinds of alloys are estimated.

* Corresponding author at: School of Materials Science and Engineering, Northeastern University, 3-11 Wenhua Road, Shenyang 110819, China.
E-mail addresses: luzheng21d@outlook.com, luz@atm.neu.edu.cn (Z. Lu).

http://dx.doi.org/10.1016/j.fusengdes.2017.06.039
0920-3796/

Table 1
The nominal chemical compositions of the alloys (wt.%).

	Cr	W	Ti	Y_2O_3	La_2O_3	CeO_2	Fe
14Y	14	2	0.3	0.3	0	0	Bal.
14L	14	2	0.3	0	0.3	0	Bal.
14C	14	2	0.3	0	0	0.3	Bal.

1. Introduction

Oxide dispersion strengthened (ODS) ferritic alloys/steels are the leading structural materials candidates for future advanced fission and fusion reactors due to excellent radiation resistance and high temperature creep strength [1,2]. These enhanced properties are mainly attributed to high number density nanoscale particles, ultrafine grains and high-density dislocations [3–5].

The microstructure of ODS alloys depends strongly on the composition and processing route. Generally, yttria is added into ODS alloys as dispersed particles because of their excellent thermal stability [6]. The addition of Ti can refine effectively yttria (Y_2O_3) and form the finer Y-Ti-rich oxides (e.g. $Y_2Ti_2O_7$, Y_2TiO_5) [7].

Recently, some alternative rare earth (RE) oxides were dispersed in the ferritic alloys such as lanthanum and cerium oxides instead of yttra [5–9]. Comparing with yttrium, the content of lanthanum is higher in common rare earth based ores [8]. Lanthanum oxides exhibited negligible solubility in Fe-based alloy [9] and relatively high thermal stability [10]. Pasebani et al. [11] studied the microstructure and mechanical properties of ODS ferritic steel with the composition of Fe-14Cr-1Ti-0.3Mo-0.5La_2O_3 by mechanical alloying (MA) and spark plasma sintering (SPS) and found that the additions of La and Ti improved the mechanical propertied and microstructural stability due to high number density Cr-Ti-La-O-rich nanoclusters. Hoffmann et al. [12] investigated the mechanical properties of different oxides (MgO, La_2O_3, Ce_2O_3 and ZrO_2) in Fe-13Cr-1W-0.3Ti ferritic steels produced by MA and hot isostatic pressing (HIP) and reported that Ce_2O_3-added alloys exhibited excellent Charpy impact property.

Although there have been some reports [11,12] about the potential application of RE oxide replacing the Y_2O_3, the precise nature of the nanoscale alternative RE oxides in ODS alloys and the influence of the addition of alternative RE oxides on the mechanical properties need to be explored in detailed. In this study, Y_2O_3, La_2O_3 and CeO_2 were added to the 14Cr ferritic matrix powders, respectively, followed by MA and SPS. The effects of Y_2O_3, La_2O_3 and CeO_2 on the microstructure and mechanical properties of 14Cr-ODS ferritic steels were investigated.

2. Experimental

High-purity elemental powders of Fe, Cr, W, Ti were mixed with nano-scale Y_2O_3, La_2O_3, CeO_2 powders, respectively, and the nominal chemical compositions were given in Table 1. The mechanical alloying was carried out in the condition of 260 rpm for 50 h with a ball to powder mass ratio of 10:1 in a high-energy planetary mill (Fritsch Pulverisette5) under an argon atmosphere. The alloys with the addition of Y_2O_3, La_2O_3 or CeO_2 were denoted as 14Y, 14L and 14C, respectively.

Dr. Sinter 1050 Spark Plasma Sintering System was used to consolidate the MA powders. The sintering was performed under constant axial pressure of 40 MPa with a pulsed direct current consisting of a 12 ms power pulse and a 2 ms intermission between pulses. The powders were heated at the speed of ~100 °C/min to 950 °C and hold for 5 min followed by cooling at the speed of ~50 °C/min. The size of SPSed samples were 30 mm in diameter and ~8 mm in thickness.

The microstructure of the ODS alloys was characterizated using a JEOL 6500F scanning electron microscope (SEM) with an electron backscattered diffraction (EBSD) and a JEOL 2100F transmission electron microscope (TEM) equipped with an energy dispersive spectrometer (EDS) system. The EBSD samples were prepared by mechanical polishing and electro-chemistry etching, and EBSD maps were acquired with a scan step of 0.03 μm. The extraction replica method was used to prepare TEM specimens in order to minimize ferromagnetic effects of the ferritic alloy matrix. The samples were mechanically polished and etched using 4% nitric acid-ethanol. The etched surfaces were coated a carbon film with a K950X coater, and then chemically etched again in the same acid solution to dissolve the matrix. The floating carbon films were retrieved on Ø 3 mm copper meshes.

The density of SPSed ODS alloys was measured according to the Archimedes drainage method. The micro-hardness (HV) was evaluated by a Vickers hardness tester 401MVDTM. The load of microhardness test is 0.98 N and the loading time is 15 s. The tensile tests were carried out using an Electric Universal Testing Machine SHIMADZU AG-Xplus in air from room temperature to 700 °C at a strain rate of 10^{-3} s^{-1}. The gauge length and cross-sectional area of tensile specimens are 10 mm and 3 mm × 1 mm, respectively.

3. Results and discussion

3.1. Nanoscale oxides

Fig. 1 shows TEM images of nanoscale oxides in three kinds of SPSed alloys and the histograms of particle size distribution. Approximately 1300 particles from ten TEM images taken from different regions were measured from each alloy. High density of nanoscale oxides are identified in Fig. 1a, c and e. The size range of these oxides is from ~2 to 20 nm. In order of 14Y, 14L and 14C, the average size of oxides increases (~6.3 nm, 7.8 nm and 11.4 nm, respectively) and the areal number density decreases (~$5.2 \times 10^{20}/m^2$, $1.7 \times 10^{20}/m^2$ and $6.6 \times 10^{19}/m^2$, respectively). The EDS spectrums of nanoscale oxides are presented in Fig. 2, which indicates that Y-Ti-Cr-rich nanoscale oxides in 14Y, La-Ti-Cr-rich nanoscale oxides in 14L and Ce-Ti-Cr-rich nanoscale oxides in 14C.

It is well-known that high density of defects (dislocations and vacancies) and supersaturated solid solution of Y (or La or Ce) are formed during MA, which provide the driving force for nanoparticle formation during the initial stage of sintering. Williams et al. [13] suggested that the formation of nanoparticles was driven by an oxidation reaction due to a low equilibrium solubility of O in the matrix and then resulted in reduction of the free energy. It is noted that Cr was found in EDS spectrums of nano size oxides. Usually, larger Cr-rich oxides (about 30 nm–200 nm) trend to precipitate mainly at grain boundaries in ODS alloys [14]. Cr enrichment in nano oxides may origin from the complicated core/shell structure oxides with Y-rich cores and Cr-rich shells. It was suggested that the presence of core/shell structures decreased the interfacial energy and favored the nucleation of the oxide particles[15,16]. The core/shell structure oxides with Y-Zr-O cores and Ti-rich shells were repoted recently in ODS-FeCrAl alloy with Zr addition, and the formation of core/shell structure oxides was contributed to dissolution-reprecipitation-diffusion mechanism [17]. Fig. 3 reveals a HRTEM image of Y-rich oxide with size of ~4 nm in 14Y. The oxide is identified to be pyrochlore-type $Y_2Ti_2O_7$ (a = 1.01 nm), which is near $[\bar{1}21]$ zone axis with [622] and $[22\bar{2}]$ atom planes and an angle 58°. Fig. 4 illustrates a La-rich oxide in 14L. Two measured atomic plane distances of [202] and $[2\bar{1}\bar{2}]$ are 3.11 Å and 2.99 Å, respectively, with an angle of 70°. This oxide is $La_2Ti_2O_7$ which has a monoclinic with a space group P21, a = 13.015 Å, b = 5.5456 Å, c = 7.817 Å,